Journal Homepage: http://ijcpe.uobaghdad.edu.iq
Iraqi Journal of Chemical and Petroleum Engineering
Vol. 25 No. 4 (December 2024) 147 – 155
EISSN: 2618-0707, PISSN: 1997-4884

Wound healing and the antimicrobial impact by using biosynthesized iron oxide nanoparticles

Abdulrahman K. Ibrahim [a, *], Rasha Al Sahlanee [a]

a Department of Biotechnology, College of Science, University of Baghdad, Baghdad, Iraq

Abstract

Chronic wound infections are a major cause of chronic wound development. This study aimed to investigate the role of Fe_2O_3 nanoparticles (Fe_2O_3 NPs) in the growth inhibition of multidrug resistant bacteria (MDR) and enhancement of human foreskin cell line migration and proliferation. For this aim, Fe_2O_3 NPs were synthesized from the bacterial extract and characterized it with UV-Vis, EDS, FTIR, AFM and FESEM assays. In addition, investigate the antibacterial effect using the well diffusion method. as well as study the cytotoxicity effect via MTT assay and the migration of cells through the scratch wound assay for human foreskin (HFF) cell line. The results confirmed the synthesis of Fe_2O_3 as the UV-Vis, which showed a peak at 288 nm; EDS showed peaks that corresponded to that of Fe_2O_3 NPs; FTIR showed absorption of functional groups belonging to bacterial extract, while FESEM revealed the irregular agglomerated shape, and AFM showed a mean diameter of 84.45 nm for Fe_2O_3 NPs. The green synthesized Fe_2O_3 revealed an antibacterial activity on MDR bacteria (Escherichia coli, Pseudomonas aeruginosa, and Staphylococcus aureus). Moreover, a significant increase in the viability of HFF cell line in dose dependent manner leading to the enhancement of these cells to migrate and proliferate to close the scratched line in 12h of incubation under the effect of these NPs. In conclusion, the findings of the current study exhibited a successful synthesized nanoparticles Fe_2O_3 from bacterial extract. These NPs presented a significant antibacterial impact against MDR bacteria. Most importantly, they showed a significant biocompatibility and promoted cell viability, migration and proliferation in HFF cells. These findings point up the capability of Fe_2O_3 as a promising treatment for wound healing applications.

Keywords: Biosynthesis; Iron Oxide nanoparticles; Antibacterial; MTT assay; scratch wound assay; Wound healing.

Received on 14/04/2024, Received in Revised Form on 05/09/2024, Accepted on 05/09/2024, Published on 30/12/2024

https://doi.org/10.31699/IJCPE.2024.4.14

1- Introduction

Among the most important technologies of this century is nanotechnology. The development of novel nanomaterials with a wide variety of applications is among the most significant advancements in the field of nanotechnology. The synthesis of safe nanomaterials with an extensive variety of applications, particularly in the biomedical and pharmaceutical domains, has drawn significant interest in recent years in research areas using bio-nanotechnology approaches [1-3].

A normal restorative response to tissue damage is wound healing. The complex series of biochemical and cellular activities interact to produce resurfacing, reconstruction, and restoration of the tensile strength of injured skin [4].

Metal nanoparticles (NPs) have gradually entered the field of wound healing with the aim of enhancing wound healing from various points of view, such as their antibacterial qualities and ability to combat antibiotic resistance. Currently, Numerous treatments for wounds that contain nanoparticles are becoming more widely available and acceptable in clinical and research settings. [5, 6].

Metals have been utilized as antibacterial agents for a very long time. Antimicrobial metal nanoparticles have emerged as the front runners in the fight against infection, especially in recent years, because of their distinctive physical and chemical characteristics [7]. Utilizing metal nanoparticles is becoming increasingly attractive because bacteria frequently show lower levels of resistance to metals [8]. Numerous studies have demonstrated the effectiveness of metals and metal oxide nanoparticles (NPs) against microorganisms. Combining antibiotics with metal nanoparticles not only decreases the use of antibiotic but also solves significant problems including drug resistance and some side effects while increasing the bactericidal effectiveness of the antibiotics [9].

Metals are becoming more important in the healing process because biofilms are necessary for the persistence of wound infections [10]. A growing number of studies have promoted wound healing and repair by using metal nanoparticles as supplementary therapeutic carriers or by using them alone.

Iron oxide nanoparticles (Fe_2O_3 NPs) are attractive for application in medical wound dressings due to their unique physicochemical characteristics. These properties include significant antioxidant and antibacterial

*Corresponding Author: Email: abdulrahman.k@sc.uobaghdad.edu.iq

capabilities, as well as the capacity to disrupt drug resistance and biofilms. The fact that Fe_2O_3 NPs are used in regenerative medicine and that many metal nanoparticles are still used in clinical settings, Their combination of antibacterial and biocompatible qualities, together with their excellent biocompatibility in both *in vitro* and *in vivo* conditions, puts them in the field of wound healing [11].

With an emphasis on Fe_2O_3 NPs and the relation between Fe_2O_3 NPs and the healing of wounds, the aim of this study is to investigate the proliferating activity of cell lines after the treatment with Fe_2O_3 NPs which might play a vital role in the accelerating wound healing process.

2- Materials and methods

2.1. Microbial strain and culture conditions

The *Pseudomonas aeruginosa* strain was grown at 37°C and 150 rpm in Brain Heart Infusion broth.

2.2. Preparation of bacterial extract

Pseudomonas aeruginosa was cultured in 1 liter of nutrient broth and then kept in an incubator shaker at 37°C for 96 hours. The supernatants were collected by centrifugation, which ran for ten minutes at 10,000 rpm. subsequently passes through a Millipore 0.22 um filter, making it ready for the synthesis of nanoparticles.

2.3. Iron oxide nanoparticle synthesis

Iron oxide nanoparticles (NPs) were produced from a *Pseudomonas aeruginosa* bacterial extract as reducing agent using a biological method [12]. an ultrasonication bath was used for 10 minutes after dissolving 5 grams of ferric chloride in 50 milliliters of the *P. aeruginosa* extracellular product solution. The flask was then placed in a darkroom on a shaker for the entire night. After that, the solution was centrifuged for 20 minutes at 8000 rpm. The resulting precipitate of iron oxide nanoparticles was washed twice with deionized water to remove any remaining cells. Finally, the nanoparticle precipitation was dried at 40 °C in an oven and stored in a dark vial as a brown substance.

2.4. Characterization of biosynthesized Fe_2O_3 NPs

2.4.1. Ultraviolet-visible (UV-Vis) spectral analysis

Using a UV-visible spectrophotometer (JASCO 670-UV), the UV-Vis spectrum analysis was performed at a resolution of 0.86 nm and in the 200–1200 nm range. Fe_2O_3 nanoparticles and bacterial extract were both analyzed in this study under various reaction conditions.

2.4.2. Fourier transform infrared (FTIR) analysis

The FTIR analysis was developed to examine the chemical bonds that existed between the atoms in the prepared materials (bacterial extract and Fe_2O_3). This specific technique was performed with a Shimadzu-IR Affinity-I spectrophotometer. In this process, the test samples are homogenized using KBr, and the FTIR spectrum is then recorded between 4000 and 400 cm^{-1} under. Prior to the recording process, potassium bromide (AR grade) was dried, and 100 mg of KBr, 1 mg of Fe_2O_3, and 100 ml of bacterial extract were combined separately. The KBr pellet was then produced under vacuum for 48 hours at 100 °C.

2.4.3. (AFM) Atomic force microscope

Fe_2O_3 nanoparticles were characterized using the atomic force spectroscopy system model (AA-3000, USA) with regard to size, surface roughness, granularity, volume distribution, and additional topography. Fe_2O_3 nanoparticles were put in a thin coating on this glass slide, and it was allowed to dry for five minutes. The slides were digitized and made available for investigation with the use of AFM scanners. As is typical, the grain size and root mean square roughness were obtained from AFM height images. The crystalline coefficient [13] was found to have been extracted during research performed by the University of Baghdad's Science College in Iraq.

2.4.4. (FESEM) Field emission scanning electron microscopy

The morphological characteristics of the produced samples (Fe_2O_3 nanoparticles) were examined using the FESEM technique. Using surface scanning, the electron beam is directed toward the material or materials under examination in the FESEM procedure to generate images. By interacting with the electron beam, the material's atoms generate singles, which allow for the analysis of surface shape and the determination of composition [14].

2.4.5. Energy dispersive X-ray (EDX) analysis

Both the sample and the apparatus used for the FESEM were used as it is. EDX analysis was used to determine the chemical purity, stoichiometry, and elemental composition of the newly synthesized nanoparticles of iron oxide.

2.5. The ability of synthetic Fe_2O_3 NPs to inhibit microorganisms

For the purpose of evaluating the antimicrobial effect of Fe_2O_3 Nanoparticles, the antibiotic-resistant bacteria *P. aeruginosa*, *E. coli*, and *S. aureus* were selected for the estimation of antibacterial activity of Fe_2O_3 NPs, and they were thankfully donated from the laboratory of pathogenic bacteria in Biotechnology Department/ college of Sciences, University of Baghdad. via the diffusion process that works nicely. 50 µl cultivated strains were streaked on nutrient agar plates overnight. A gel puncher was used to make a 5 mm diameter well in the plates. Varying concentrations (100, 50, 25, 12.5, 6.25, and 3.125

mg/ml) of Fe_2O_3 nanoparticles were added to the wells. The process was done with each of the three bacterial strains. In an incubator set at 37ºC, the plates were incubated for two days. A zone of clearance analysis was used to assess the antibacterial efficacy of iron oxide nanoparticles [15].

2.6. Cytotoxicity (MTT) assays

Using the MTT test (3-(4,5-dimethylthiazol-2-yl)-2,5-diphenyltetrazolium bromide), the anticancer effects of Fe_2O_3 NPs were assessed against MCF7 and HFF cell lines. In order to maintain MCF7 and HFF cell lines, 10.0% fetal bovine serum in Dulbecco's Minimal Essential Medium (DMEM) (Himedia) was augmented with 100 mg/ml of streptomycin and 100.0 U/ml of penicillin. After that, for 24 hours, the cells were incubated at 37 °C with 5% CO_2. To evaluate the vitality of the cells, MCF7 and HFF cells (1 × 105 cells/well) were exposed to five distinct doses of Fe_2O_3 NPs (25, 75, 150, 300, and 500 µg/mL) and allowed to incubate for 24h. MTT (10 µL) has been added to each well. after the cells had been cultured for 24h, and the wells were then incubated for an additional 4h at 37 °C. After carefully discarding the supernatant containing MTT medium, each well received 200 µL of dimethyl sulfoxide (DMSO) in order to dissolve the formazan crystals. The absorbance was determined with a micro-plate reader at 570 nm [16, 17]. The formula was utilized to calculate the proportion of viable cells in comparison to control wells that contained cell culture media free of Fe_2O_3 NPs. The formula for calculating cell viability (%) is (Abs of the test cell compared to the Abs of control cell) x 100.

2.7. In vitro test for scratches

According to the previously published protocol [18], the Fe_2O_3 NPs in vitro scratch test was carried out. To perform this, 24 well plates were filled with DMEM medium for seeding. containing HaCaT, KMST-6, and CHO cells (2×105 cell/mL), and the plates were then incubated under standard conditions. Using a sterile pipette tip, a scratch was formed as soon as a homogeneous monolayer of cells was formed by the cell growth. Excess detached cells were then washed away with DMEM (without FBS). Then the cells were treated with 100 µg/mL of sterilized Fe_2O_3 NPs in FBS-free DMEM. In the control group, cells remained untreated. Axio Observer 5, Zeiss, Germany: Bright field microscopy was used to take images after 0, 12, 24, and 48 hours of treatment. Additionally, ImageJ (version 1.52e) software was used to measure the scratch's initial and final widths. The following formula was used to get the scratch shrinking percentage: (Original width – Final width)×100/Original width is the scratch shrinking percentage.

3- Results and discussion

3.1 .UV-visible analysis

An ultraviolet-visible spectrometer was used to examine the optical characteristics of nanoparticles. At room temperature, in the nano range, the absorbance of the material is shown in Fig. 1. Thus, a peak with a wavelength of 288 nm was confirmed [19].

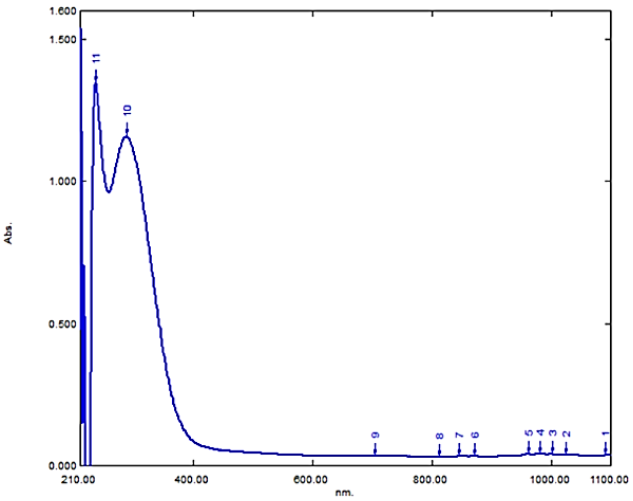

Fig. 1. The UV-VIS of iron oxide NPs synthesized using bacterial extract

3.2. FESEM analysis

Using FE-SEM, 110kx magnification pictures of the material were taken. focused on Fig. 2. The entire sample consists of Fe_2O_3 nanocluster centers with some irregular agglomerated nanoparticles [20].

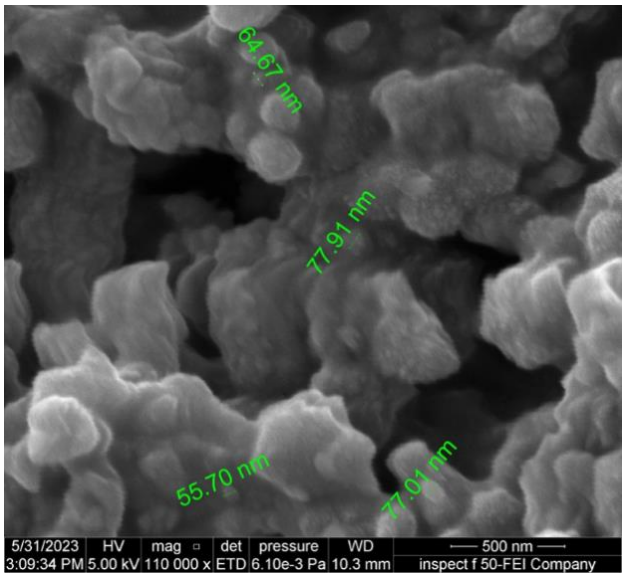

Fig. 2. FE-SEM image of Fe2O3 nanoparticles using bacterial extract as a reducing agent

3.3. EDX analysis

For further confirmation of the composition of the obtained products, an EDX examination was performed. The products of 4 hours of calcination at 800°C are made of iron, as seen in Fig. 3. The electric latex of the EDX sample holder is responsible for the C peak in the spectrum.

3.4. FT-IR analysis

The functional groups of the nanoparticles have been identified using the FTIR spectra. The FTIR absorption spectra of biologically produced nanoparticles are shown in Table 1. A strong peak at (3461.99 – 3373.27 cm^{-1}) was seen as a result of the OH stretching mode. O-H bend, or crystallographic H2O molecules, were indicated by the peak characteristics that occurred at (1647.10 cm^{-1}). The Fe–O band and Fe–O–F skeleton frequency were indicated by the wide peaks at (424.31 cm^{-1}) and (516.89 cm^{-1}), respectively [20].

3.5. AFM analysis

Atomic force microscopy was used to examine the surface shape formation of the Fe_2O_3 NPs, demonstrating that the NPs are 2D and 3D [20]. Fig. 4. Fe_2O_3 NPs that have been biosynthesized are spherical, as shown by AFM images. AFM Fig. 5. was also used to measure the average diameter of 84.45 nm.

3.6. Antimicrobial activity of iron oxide Nps against multidrug resistant bacteria

Fe_2O_3 NPs suspensions were tested for their relative antibacterial activity against pathogenic isolates, including *Escherichia coli*, *Pseudomonas aeruginosa*, and *Staphylococcus aureus*, the inhibition zone was evaluated on nutrient agar plates in this study. Table 2 shows results from the testing of six Fe_2O_3 NPs suspensions at concentrations of 100, 50, 25, 12.5, 6.25, and 3.125 mg/ml. According to the results, the isolates of gram-negative bacteria (*E. coli* and *P. aeruginosa)* the maximal E. Coli inhibitory zones at 100 mg/ml of iron oxide nanoparticle concentration was 15 mm, Whereas the concentration of the minimal inhibition zones was 6.25 mg/ml. and for *P. aeruginosa* were 26 mm at a concentration 100 mg/ml of iron oxide nanoparticles, Whereas the minimum inhibition zones were located at 6.25 mg/ml and no inhibition at the concentrations of (3.125 mg/ml) of Fe_2O_3 NPs concentrations, the inhibition zone depended on the concentration of iron oxide nanoparticles. It has previously been noted that the structural composition of the cell membrane, more especially the thickness of the peptidoglycan layer, determines whether nanoparticles have antibacterial effects on both Gram-positive as well as Gram-negative bacteria [21]. While Gram-negative bacteria's cell wall has a thinner polysaccharide layer and showed a significant bactericidal effect, to allow Fe_2O_3 NPs to pass through their rigid cell membrane, gram-positive microbes have a thick layer of peptidoglycan composed of linear polysaccharide chains cross-linked with short peptides. and preventing the formation of an inhibition zone. These results are the same as the results [22] that the nanoparticles have bactericidal activity toward both Gram-positive and Gram-negative bacteria.

3.7. Effect of Fe_2O_3 NPs on cell lines

The cytotoxicity of Fe_2O_3 NPs was investigated by measuring viability using MTT shows the viability results examined by MTT colorimetric assay of the MCF7 and HFF. In the case of HFF as well as the MCF7 cell lines, their viability increased in a dose-dependent manner in the presence of Fe_2O_3 NPs. The highest growth was found at a concentration of 75 µg/mL of Fe_2O_3 NPs for MCF7 cell line and at 300 µg/mL for HFF cell line, while at 25 µg/mL concentration lower cells were grown for both MCF7 and HFF cell lines, Fig. 6, Iron oxide nanoparticles showed high growth rate towards MCF7 and HFF cell line

Weight % Error	Weight %	Atomic % Error	Atomic %	Element
0.4	18.1	0.8	34.7	C
0.5	30.7	0.7	44.2	O
0.4	51.3	0.2	21.1	Fe

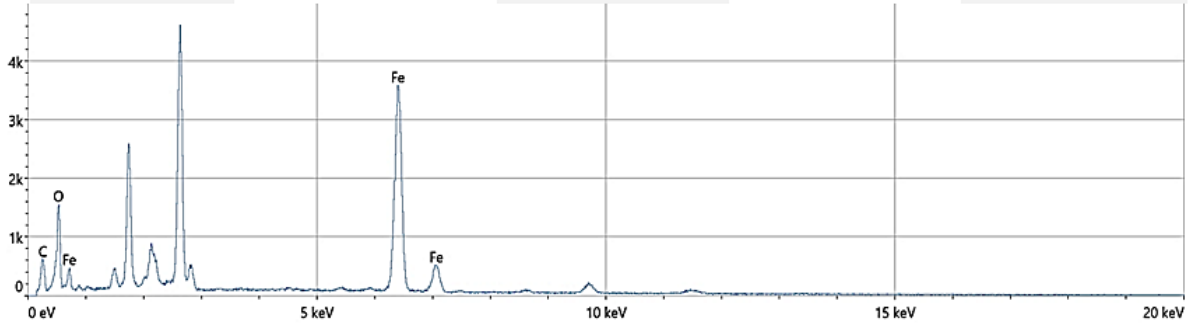

Fig. 3. The EDX analysis of iron oxide NPs synthesized using bacterial extract

Table 1. FTIR of iron oxide NPs

Type of compound	Frequency of Absorption (cm-1)	bonds	Compound class of functional groups
Bacterial Extract	3409.91-3307.69	O-H stretch	Alcohol and hydroxyl compound
	1652.88	O-H stretch	Alkenyl
	1402.15	O-H bend	Tertiary alcohol
Ferric chloride	3390.63–3371.34	O-H stretching	Alcohol
	1610.45-1585.38	C=C stretching	cyclic alkene
Iron oxide NPs	3461.99-3373.27	O-H stretching	Alcohol
	1647.10	C=N stretching	imine / oxime
	1099.35-1083.92	C-N stretching	amine
	516.89-424.31	Fe-O band as well as Fe-O-Fe skeletal	Metal oxide

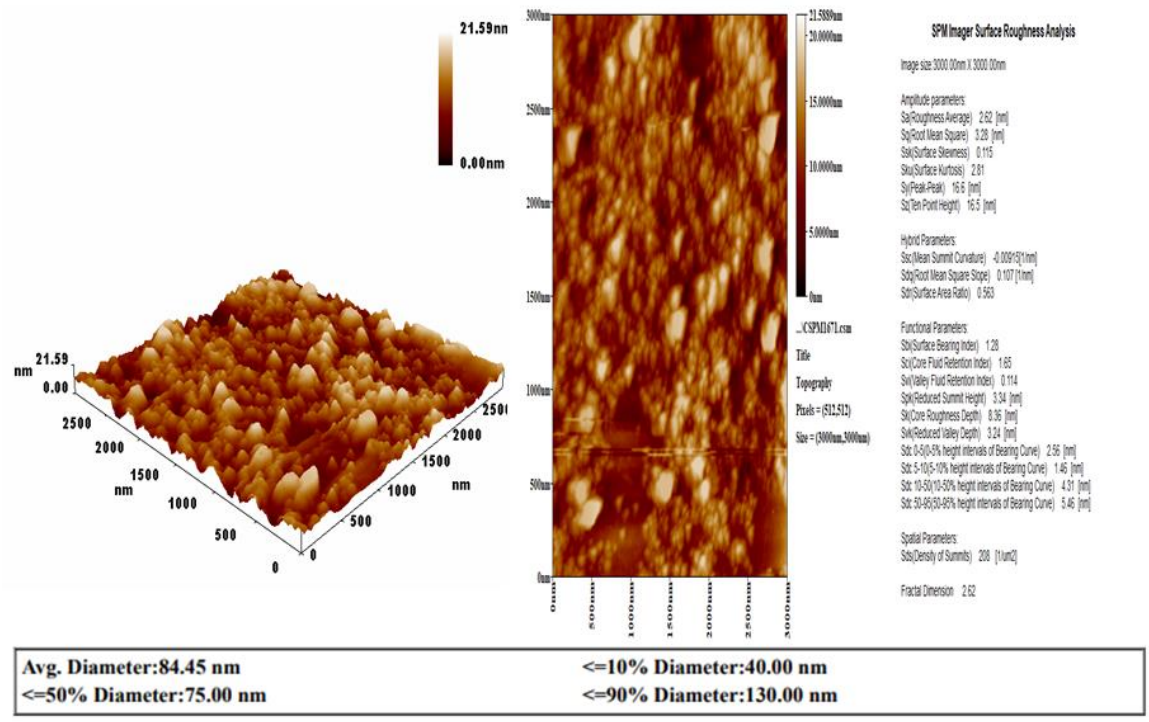

Fig. 4. Nanoparticle Fe_2O_3 shown in 2D and 3D using atomic force microscopy

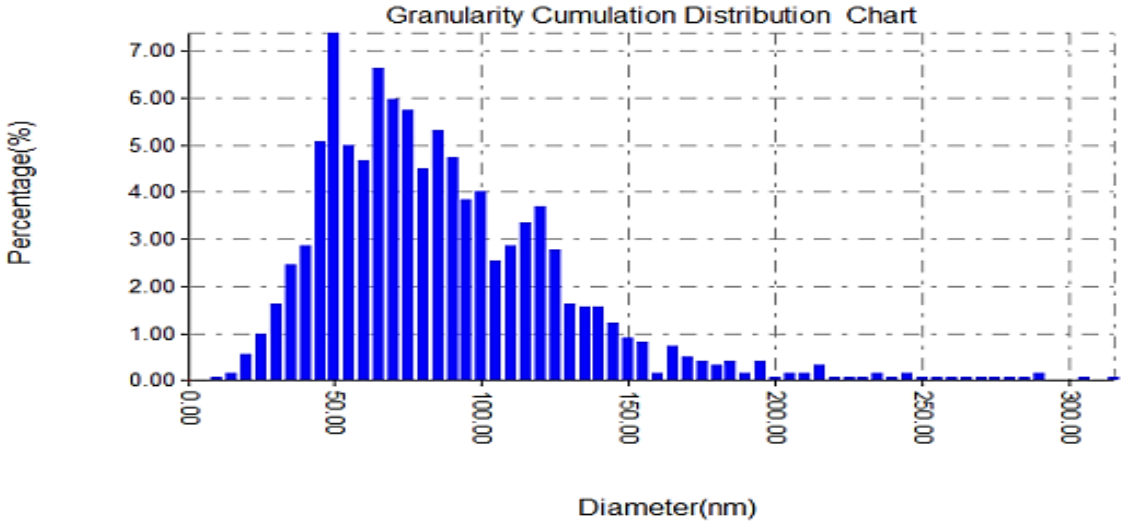

Fig. 5. Fe_2O_3 Nanoparticles average size synthesized using bacterial extract

Table 2. Antibacterial activity test of iron oxide nanoparticles on some multi-drug resistant bacteria

NO	Iron oxide NPS con. (mg/ml)	Inhibition zone (Diameter, mm)		
		Staphylococcus aureus	P. aeruginosa	E. Coli
1	100	24	26	15
2	50	19	25	14
3	25	15	15	9
4	12.5	12	12	5
5	6.25	9	9	1
6	3.125	No inhibition zone	No inhibition zone	No inhibition zone

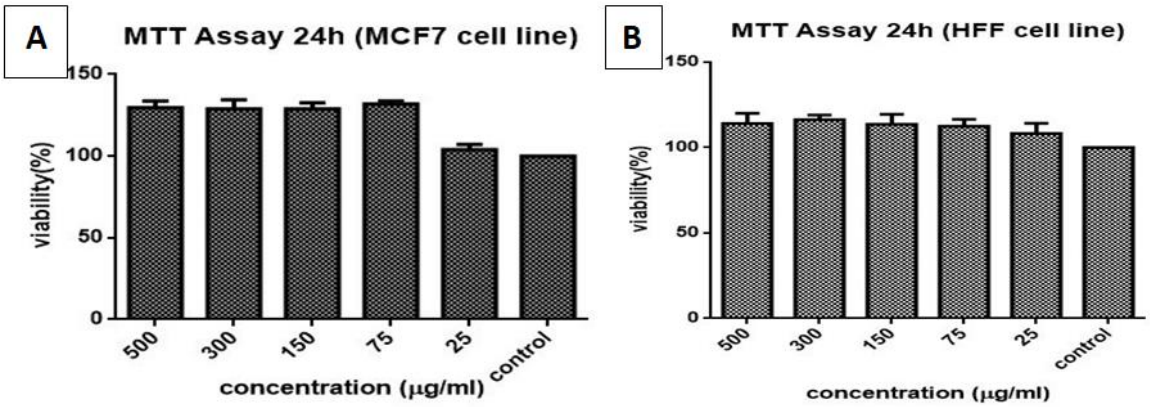

Fig. 6. Cytotoxic effect of iron oxide against A: MCF7 (human breast cancer) and B: cell lines of HFF (human foreskin fibroblasts) after incubation at 37ºC for 72 hours. using *: p-value ≤ 0.05- significant

3.8. Application of Fe_2O_3NPs as wound healing

Burns and other complex wounds need the use of antimicrobial and wound-healing substances. The in vitro scratch test is a helpful technique for examining the potential for drugs or nanoparticles to promote wound healing due to it helps to understanding how cells migrate and proliferate during the healing process [18]. This test can definitively determine if a specific substance or a compound speed up or decreases the speed at which cells migrate and proliferate. Our results as shown in the Fig. 7 revealed that the HFF cell line increased in proliferation rate after 12h of Fe_2O_3 NPs treatment and completely filled the scratch line after 24h and continue of growth to form complete monolayer at the end of experiment at 48h, while the untreated cells showed a slow proliferation rate and the confluency of monolayer appear only in 48h. these results comes in agreement with previous study [23] suggesting that the iron oxide nanoparticles enhance cells migration to the injury sites.

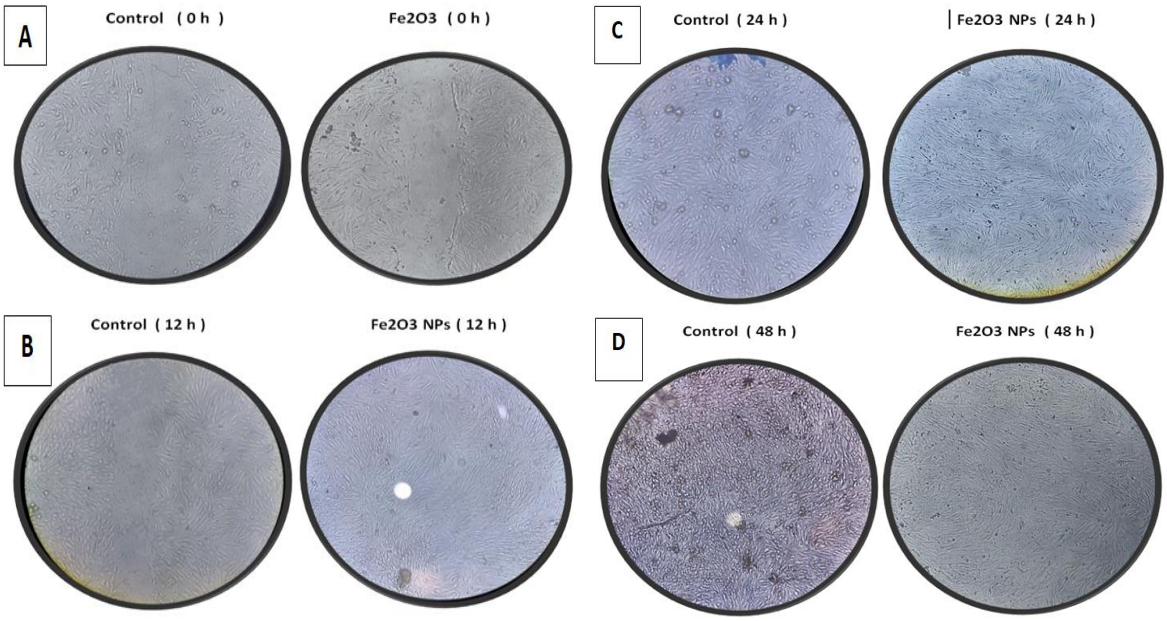

Fig. 7. Scratch assay of HFF cell line with 100 µg/mL Fe_2O_3 NPs present. After A:0, B:12, C:24, and D: 48 hours of incubation, bright-field images of the cells treated with Fe_2O_3 NPs and the negative control (untreated cells) were obtained

4- Conclusion

Fe_2O_3 nanoparticles concordantly include both the antibacterial activity for MDR bacteria and enhance human cells migrations, potentially gives important need for new wound healing treatment in the clinical practice to manage the bacterial infections of wound and accelerate cloture of wounds. The use of biological methods for synthesizing Fe_2O_3 NPs, such as using bacterial extracts, is environmentally friendly and cost-effective compared to traditional chemical synthesis methods. The biological molecules in the extracts can also provide functionalization to the Fe_2O_3NPs, enhancing their stability and effectiveness. While biosynthesis is advantageous, scaling up the production of Fe_2O_3 NPs while maintaining consistency and quality remains a challenge. Further research is needed to optimize the biosynthesis process for large-scale production. By addressing both the wound healing and antimicrobial impacts of biosynthesized iron oxide nanoparticles, this discussion highlights their potential as a dual-function therapeutic agent, providing insights into their mechanisms and future application prospects.

References

[1] S. Ahmad, S Munir, N Zeb, A Ullah, B Khan, J Ali, M Bilal, M Omer, M Alamzeb, SM Salman, "Green nanotechnology: A review on green synthesis of silver nanoparticles—An ecofriendly approach," International journal of nanomedicine, pp. 5087-5107, 2019. https://doi.org/10.2147/IJN.S200254

[2] S. Bayda, M. Adeel, T. Tuccinardi, M. Cordani, and F. Rizzolio, "The history of nanoscience and nanotechnology: from chemical–physical applications to nanomedicine," Molecules, vol. 25, no. 1, p. 112, 2019. https://doi.org/10.3390/molecules25010112

[3] J. K. Patra and K.-H. Baek, "Green nanobiotechnology: factors affecting synthesis and characterization techniques," Journal of Nanomaterials, vol. 2014, pp. 219-219, 2015. https://doi.org/10.1155/2014/417305

[4] T. Morikawa, "Tissue sealing," The American journal of surgery, vol. 182, no. 2, pp. S29-S35, 2001. https://doi.org/10.1016/S0002-9610(01)00774-7

[5] M. A. Khan and M. Mujahid, "A review on recent advances in chitosan based composite for hemostatic dressings," International journal of biological macromolecules, vol. 124, pp. 138-147, 2019. https://doi.org/10.1016/j.ijbiomac.2018.11.045

[6] A. Sathiyaseelan, K. Saravanakumar, A. V. A. Mariadoss, and M.-H. Wang, "Antimicrobial and wound healing properties of FeO fabricated chitosan/PVA nanocomposite sponge," Antibiotics, vol. 10, no. 5, p. 524, 2021. https://doi.org/10.3390/antibiotics10050524

[7] N. Beyth, Y. Houri-Haddad, A. Domb, W. Khan, and R. Hazan, "Alternative antimicrobial approach: nano-antimicrobial materials," Evidence-based complementary and alternative medicine, vol. 2015, 2015. https://doi.org/10.1155/2015/246012

[8] H. A. Hemeg, "Nanomaterials for alternative antibacterial therapy," International journal of nanomedicine, pp. 8211-8225, 2017. https://doi.org/10.2147/IJN.S132163

[9] A. M. Allahverdiyev, K. V. Kon, E. S. Abamor, M. Bagirova, and M. Rafailovich, "Coping with antibiotic resistance: combining nanoparticles with antibiotics and other antimicrobial agents," Expert review of anti-infective therapy, vol. 9, no. 11, pp. 1035-1052, 2011. https://doi.org/10.1586/eri.11.121

[10] S.-f. Shi, J Jia, X Guo, Y Zhao, D Chen, Y Guo, X Zhang, "Reduced Staphylococcus aureus biofilm formation in the presence of chitosan-coated iron oxide nanoparticles," International journal of nanomedicine, pp. 6499-6506, 2016. https://doi.org/10.2147/IJN.S41371

[11] Y. Gong, Y. Ji, F. Liu, J. Li, and Y. Cao, "Cytotoxicity, oxidative stress and inflammation induced by ZnO nanoparticles in endothelial cells: interaction with palmitate or lipopolysaccharide," Journal of Applied Toxicology, vol. 37, no. 8, pp. 895-901, 2017. https://doi.org/10.1002/jat.3415

[12] R. H. Ali, M. R. Majeed, and H. A. Jasim, "Determination of vasicine alkaloid efficacy as inhibitor to the activity of protease produced by a clinical isolate of Pseudomonas aeruginosa," Iraqi Journal of Science, pp. 1237-1246, 2018.

[13] H. Yang, Atomic force microscopy (AFM): Principles, modes of operation and limitations. Nova Science Publishers, Incorporated, 2014.

[14] J. Pawley, "The development of field-emission scanning electron microscopy for imaging biological surfaces," SCANNING-NEW YORK AND BADEN BADEN THEN MAHWAH-, vol. 19, pp. 324-336, 1997.

[15] A. Rajan, E. Cherian, and G. Baskar, "Biosynthesis of zinc oxide nanoparticles using Aspergillus fumigatus JCF and its antibacterial activity," International Journal of Modern Science and Technology, vol. 1, no. 2, pp. 52-57, 2016.

[16] P. Rathinaraj, K. Lee, Y. Choi, S.-Y. Park, O. H. Kwon, and I.-K. Kang, "Targeting and molecular imaging of HepG2 cells using surface-functionalized gold nanoparticles," Journal of Nanoparticle Research, vol. 17, pp. 1-12, 2015. https://doi.org/10.2147/BCTT.S69834

[17] P. Chen, H. Wang, M. He, B. Chen, B. Yang, and B. Hu, "Size-dependent cytotoxicity study of ZnO nanoparticles in HepG2 cells," Ecotoxicology and environmental safety, vol. 171, pp. 337-346, 2019. https://doi.org/10.1016/j.ecoenv.2018.12.096

[18] M. Felder, B Trueeb, AO Stucki, S Borcard, JD Stucki, B Schnyder, T Geiser, OT Guenat, "Impaired wound healing of alveolar lung epithelial cells in a breathing lung-on-a-chip," Frontiers in bioengineering and biotechnology, vol. 7, p. 3, 2019. https://doi.org/10.3389/fbioe.2019.00003

[19] V. Vorobeva, N. Domracheva, M. Gruzdev, and A. Pyataev, "Optical properties and photoinduced superparamagnetism of γ-Fe2O3 nanoparticles formed in dendrimer," Materials Science in Semiconductor Processing, vol. 38, pp. 336-341, 2015. https://doi.org/10.1016/j.mssp.2014.09.045

[20] L. Yaaqoob, "Evaluation of the biological effect synthesized iron oxide nanoparticles on Enterococcus faecalis," Iraqi Journal of Agricultural Sciences, vol. 53, no. 2, pp. 440-452, 2022. https://doi.org/10.36103/ijas.v53i2.1552

[21] S. Shrivastava, T. Bera, A. Roy, G. Singh, P. Ramachandrarao, and D. Dash, "Characterization of enhanced antibacterial effects of novel silver nanoparticles," Nanotechnology, vol. 18, no. 22, pp. 225103-225500, 2007. https://doi.org/10.1088/0957-4484/18/22/225103

[22] J. Yoonus, R. Resmi, and B. Beena, "Evaluation of antibacterial and anticancer activity of green synthesized iron oxide (α-Fe2O3) nanoparticles," Materials Today: Proceedings, vol. 46, pp. 2969-2974, 2021. https://doi.org/10.1016/j.matpr.2020.12.426

[23] S. Öksüz, MS Alagöz, H Karagöz, Z Küçükodac, E Karaöz, G Duruksu, G Aksu, "Comparison of treatments with local mesenchymal stem cells and mesenchymal stem cells with increased vascular endothelial growth factor expression on irradiation injury of expanded skin," Annals of Plastic Surgery, vol. 75, no. 2, pp. 219-230, 2015. https://doi.org/10.1097/SAP.0000000000000574

التئام الجروح وتأثير مضادات الميكروبات باستخدام جزيئات أكسيد الحديد النانوية المصنعة حيويا

عبد الرحمن خليل ابراهيم [١، *]، رشا طالب عبد الله [١]

١ قسم التقنيات الاحيائية، كلية العلوم، جامعة بغداد، بغداد، العراق

الخلاصة

تعد التهابات الجروح المزمنة سببًا رئيسيًا لتطور الجروح المزمنة. هدفت دراستنا إلى التحقق من دور الجسيمات النانوية (IONPs) Fe_2O_3 في تثبيط نمو البكتيريا المقاومة للأدوية المتعددة (MDR) وتعزيز هجرة خط خلايا القلفة البشرية وانتشارها. ولتحقيق هذا الهدف، تم تصنيع IONPs من المستخلص البكتيري وتم توصيفها بمقاييس UV–vis وEDS وFTIR وAFM وFESEM. وتم التحقق من التأثير المضاد للبكتيريا باستخدام طريقة الانتشار الجيد. وبالإضافة إلى ذلك، تم التحقق ايضاً في تأثير السمية الخلوية عن طريق تقنية MTT واختبار هجرة الخلايا لخط خلايا القلفة البشرية (HFF) من خلال طريقة (تقنية) الجرح المخدوش. وتم التأكد من تخليق Fe_2O_3 من خلال نتائج العديد من تقنيات التوصيف بالاعتماد على شكل الاشعة فوق البنفسجية المرئية، والتي أظهرت ذروتها عند ٢٨٨ نانومتر؛ أظهر EDS قممًا تتوافق مع تلك الخاصة بـ Fe_2O_3 NPs؛ أظهر FTIR امتصاصاً للمجموعات الوظيفية التي تنتمي إلى المستخلص البكتيري، بينما أظهر FESEM الشكل المتكتل غير المنتظم وأظهر AFM متوسط قطر ٨٤ نانومتر لـ Fe_3O_4 NPs. أظهرت الجسيمات النانوية التي تم تخليقها نشاطًا مضادًا للعديد من بكتيريا MDR وزيادة نمو خط الخلية بطريقة تعتمد على الجرعة مما يؤدي إلى تعزيز هذه الخلايا للهجرة والتكاثر لإغلاق الخط المخدوش خلال ١٢ ساعة من الحضانة تحت تأثير هذه NPs. تشير النتائج التي توصلنا إليها إلى أن الجسيمات النانوية التي تم تخليقها تمتلك علاجًا واعدًا لالتهابات الجروح والشفاء والتغلب على المقاومة البكتيرية.

الكلمات الدالة: التخليق الحيوي، جسيمات أكسيد الحديد النانوية، مضاد للبكتيريا، فحص MTT، فحص الجرح المخدوش، التئام الجروح.